scientific reports

Check for updates

OPEN

The synergistic antitumour effect of Carrimycin combined with 5-fluorouracil on colorectal cancer

Chaoyue Shi[1], Xiao Ma[1], Ruixue Zhang[1], Zhenhua Lin[1] & Xianchun Zhou[1,2]✉

5-Fluorouracil (5-FU)-based chemotherapy often leads to drug resistance and adverse reactions in individuals with colorectal cancer (CRC). Carrimycin (CAM), a drug with notable antitumour effects across various tumour types, including hepatocellular carcinoma, glioblastoma, and small-cell lung carcinoma, offers an alternative owing to its limited side effects. Combination therapy is a common strategy to mitigate the negative effects of 5-FU and enhance its therapeutic efficacy. This study aimed to investigate the potential synergistic antitumour effects of CAM and 5-FU on HCT-15 and HT-29 CRC cell lines. Using computational analysis, we identified and quantified the synergistic effects of CAM and 5-FU. The combination therapy significantly outperformed 5-FU alone in inhibiting cell proliferation, colony formation, cell cycle progression, and migration. Additionally, it markedly increased the levels of reactive oxygen species and induced DNA damage. Furthermore, RNA-seq analysis revealed that the JNK and p38 MAPK signalling pathways were activated by this combination. In addition, the synergistic effects of the combination therapy were validated in a mouse subcutaneous tumour graft model. In conclusion, CAM enhances the sensitivity of CRC cells to 5-FU both in vitro and in vivo, suggesting its potential as a promising candidate for combination cancer therapy.

Keywords Carrimycin, DNA damage response, Cell cycle, Reactive oxygen species, MAPK pathway

Despite the notable advancements in early screening, surgical techniques, and chemotherapy regimens, colorectal cancer (CRC) remains the second leading cause of cancer-related deaths. Notably, there is an annual increase of 1–2% in the incidence of CRC among patients aged < 55 years[1]. The 5-year survival rate of patients with advanced or metastatic CRC after surgery and chemotherapy is < 20%[2]. 5-Fluorouracil (5-FU) has extensive applications in clinical settings for the treatment of CRC[3]. At present, 5-FU is usually combined with other cytotoxic drugs, such as irinotecan or oxaliplatin, to boost its therapeutic effects, however, its application remains limited owing to severe systemic toxicity and drug resistance[4,5]. The conventional chemotherapy is limited by suboptimal therapeutic efficacy and significant treatment-related toxicities, the development of more efficacious and innovative therapeutic modalities represents an urgent unmet clinical need in contemporary oncology practice, particularly for refractory malignancies and treatment-resistant phenotypes.

Carrimycin (CAM), a novel recombinant macrolide antibiotic primarily composed of isovalerylspiramycin I, II, and III, exerts its therapeutic effects by targeting the 50 S ribosomal subunit to inhibit protein synthesis[6]. Previous studies have shown that CAM has powerful antiviral and anti-inflammatory properties and regulates the immune response[7,8]. Given that tumor cells generally have a high capacity for replication and metabolism, and there is a close relationship between the occurrence of colorectal tumors and inflammation, the mechanism of action of CAM makes it potentially valuable for antitumour therapy[9]. Besides, CAM shows promise in preventing the growth of tumour cells in liver, oral, lung, and brain cancers[10–14]. A phase III clinical trial indicated that CAM is safe and effective at a low oral dose; it has few adverse effects, no secondary resistance, good bioavailability, and high biosafety[15]. These properties make CAM a strong candidate for exploring new drug combination regimens and chemosensitizer. However, the antitumor efficacy of CAM in CRC remains unexplored. Therefore, the present study aimed to investigate the therapeutic potential of CAM in CRC treatment and evaluate its feasibility in combination regimens, thereby providing new insights into CRC treatment strategies.

The JNK and p38 MAPK signalling pathways are activated by oxidative stress, cytokines, and ultraviolet light, and they play a significant role in the regulation of apoptosis[16]. Anticancer drugs, such as cyclophosphamide and oxaliplatin, trigger apoptosis via the p38 MAPK pathway, and cisplatin activates JNK in ovarian cancer cells[17–19]. In CRC cells, herbal extracts, such as deoxybouvardin, isolinderalactone, and echinatin, induce apoptosis through JNK/p38 MAPK signaling[20–22]. Yu et al. showed that aldehyde dehydrogenase inhibition activates these

[1]Central Laboratory, Yanbian University Hospital, Yanji, Jilin, China. [2]Yanbian University Hospital, Yanji 133000, Jilin Province, China. ✉email: xczhou@ybu.edu.cn

pathways in CRC, leading to apoptosis and DNA damage[23]. Therefore, targeting the JNK/p38 MAPK pathway may be a promising CRC treatment strategy.

Our study aim to investigate the effect of the combined application of CAM and 5-FU in vivo and in vitro, and to evaluate the potential of CAM as a chemosensitiser when used in combination with 5-FU. We determined the effective drug concentrations and revealed the specific molecular mechanisms. This is the first study to propose the macrolide antibiotic CAM as a low toxicity chemosensitiser in CRC treatment, providing new insights into the development of safer and more effective CRC treatment regimens.

Results

Synergistic effects of CAM and 5-FU increase CRC cytotoxicity

To investigate the potential of CAM as an anticancer sensitiser, a CCK-8 assay was performed to measure the biological effects of CAM in SW-620, SW-480, DLD, RKO, HCT-15, and HT-29 cell lines, and a dose-response curve was drawn (Fig. 1A, and supplementary Fig. S1A). The CAM concentration gradients were 0, 2, 4, 8, 16, and 32 μg/mL; the half-maximal inhibitory concentration (IC_{50}) values are shown in supplementary Fig. S1B. HCT-15 and HT-29 cells, which were the most sensitive to CAM, were selected for subsequent experiments (supplementary Fig. S1B). Cytotoxicity of 5-FU was assessed using the same technique (Fig. 1B). Both CAM and 5-FU exhibited dose-dependent antiproliferative effects. To explore the synergistic effects of CAM and 5-FU, the SynergyFinder online tool was used to calculate highest single-agent (HSA) synergy scores across a range of concentration gradients. The HSA synergy scores for the HCT-15 and HT-29 cell lines were 17.15 and 17.4,

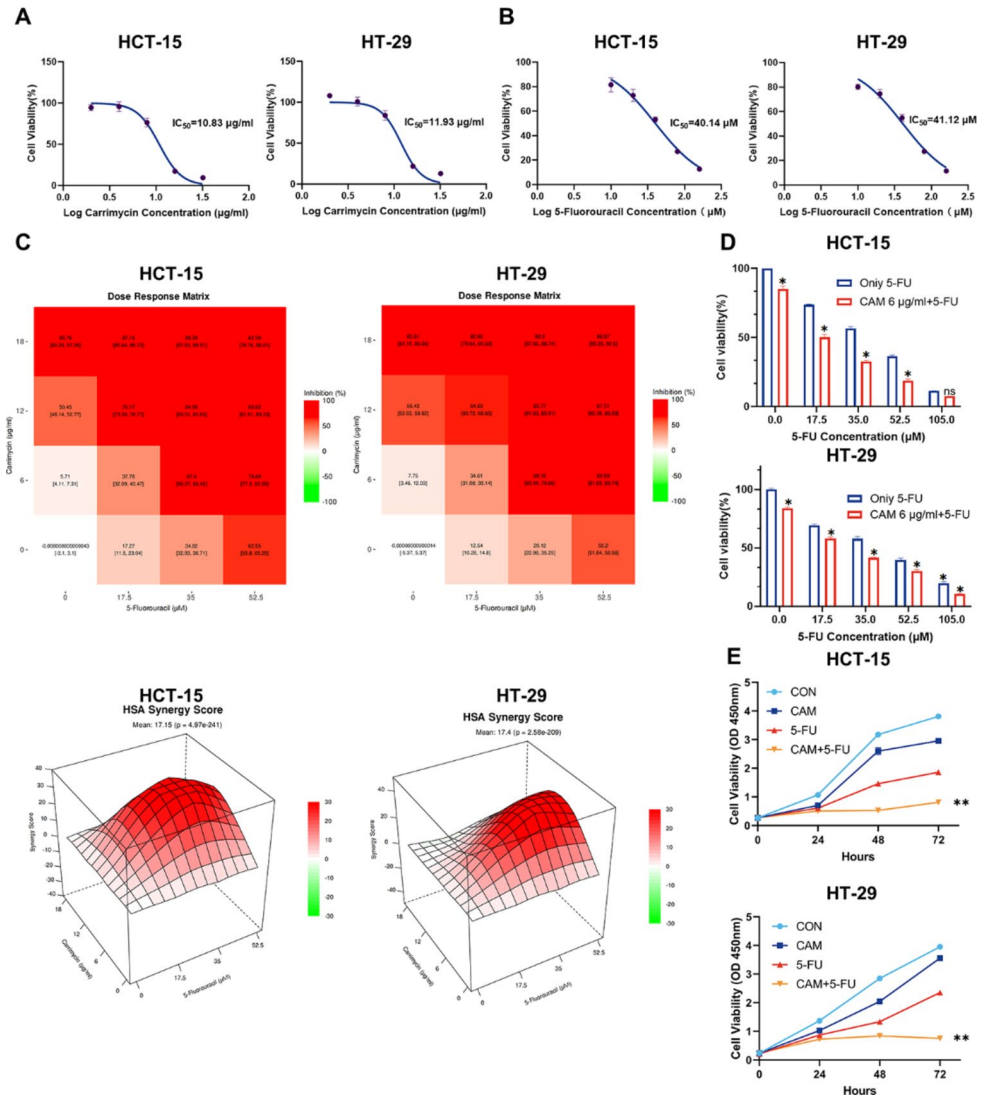

Fig. 1. Low-dose CAM enhances 5-FU's cytotoxicity in CRC cells. (**A**-**B**) cell viability. (**C**) Drug combination heatmaps with HAS Synergy scores from Synergyfinder; scores > 0 indicate synergy, > 10 indicate strong synergy. (**D**) Cell viability after 24 h treatment with CAM (6 μg/ml) and different concentration gradients of 5-FU; (**E**) Cell viability after treatment with CAM (6 μg/ml) and 35 μM of 5-FU for 24, 48, 72 h. Error bars show SEM. $^{*}P < 0.05$, $^{**}P < 0.01$, $^{***}P < 0.001$.

respectively. CAM and 5-FU exhibited a strong synergistic effect in reducing tumour growth. Moreover, a CAM concentration of 6 μg/ml was identified as the threshold for optimal synergy (Fig. 1C), and this concentration was combined with varying concentrations of 5-FU. The results indicated that a 5-FU concentration of 35 μM, which is lower than its IC_{50} value, is optimal for achieving synergistic antiproliferative effects (Fig. 1D). Treatment with 6 μg/mL CAM and 35 μM 5-FU for 72 h significantly reduced the growth rates of CRC cells (Fig. 1E). These results demonstrated that even at doses far below the IC_{50}, CAM can synergistically enhance the cell-killing effects of 5-FU in CRC. Colony formation assays revealed that CAM + 5-FU markedly suppressed the proliferation capacity of CRC cells ((supplementary Fig. S2A, B). Similarly, Ethynyl-2-deoxyuridine (EdU) incorporation assays showed a significant decrease in the EdU incorporation rate of the CAM + 5-FU group compared to the individual treatments. This result highlighted the potent synergistic antiproliferative effects of the combination (supplementary Fig. S2C, D).

CAM increased 5-FU-induced apoptosis and DNA damage

To investigate the effect of CAM + 5-FU on cellular apoptosis, a flow cytometry analysis was performed. Low doses of CAM or 5-FU alone caused a slight increase in apoptosis, whereas the CAM + 5-FU combination resulted in a significantly higher apoptosis rate (Fig. 2A, B). This combination also significantly increased the expression levels of cleaved PARP1 and CYC1 and the Bax/Bcl-2 ratio in CRC cells. Additionally, compared to treatment with 5-FU alone, the combination therapy increased the levels of P-H2AX and decreased the levels of RAD51. This result indicated increased DNA damage and inhibition of the DNA repair process (Fig. 2C,

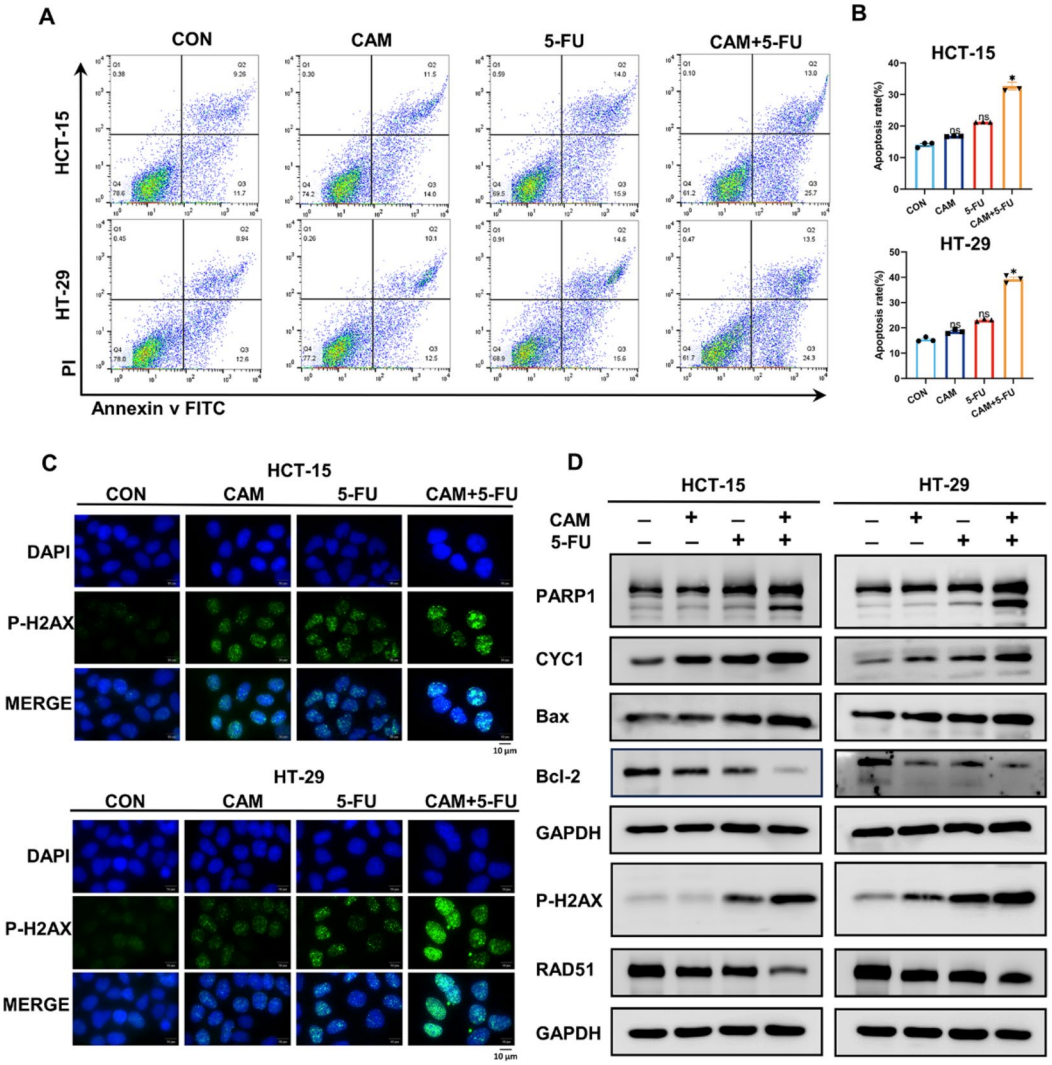

Fig. 2. The combination of CAM and 5-FU induced apoptosis and increased DNA damage. (**A**) Apoptosis flow cytometry plots. (**B**) Quantification of apoptotic. (**C**) Immunofluorescence staining. Scale bar, 10 μm. (**D**) The levels of PARP1, CYC1, P-H2AX, RAD51, Bax, and Bcl-2 proteins were assessed via western blot. GAPDH was utilized as a loading control. Error bars represent the SEM. $^{*}P < 0.05$; $^{**}P < 0.01$; $^{***}P < 0.001$. CYC1, cytochrome c-1.

D). Overall, these results demonstrated that the CAM + 5-FU combination promotes both apoptosis and DNA damage, suggesting its potential as an effective therapeutic strategy.

CAM combined with 5-FU enhanced cell cycle arrest

To investigate the effects of CAM in combination with 5-FU in vitro, flow cytometry was performed to analyse the cell cycle. We treated CRC cells with CAM (10, 15, and 20 μg/ml), and the percentage of cells in the G0/G1 phase increased in a dose-dependent way (Fig. 3A, B). CAM enhanced G1-phase arrest, whereas 5-FU primarily induced S-phase arrest. The combined CAM + 5-FU treatment further disrupted the cell cycle progression by significantly reducing the proportion of G2 cells (Fig. 3C, D). Gene set enrichment analysis (GSEA) revealed a significant enrichment of cell cycle-related genes in response to the combination treatment. CAM + 5-FU markedly elevated the protein expression of P21 and P27 proteins, reduced the expression of cyclin D1 and cyclin A2 (Fig. 3E, F). These results indicated that CAM + 5-FU treatment effectively inhibited CRC cell cycle progression by targeting distinct cell cycle phases.

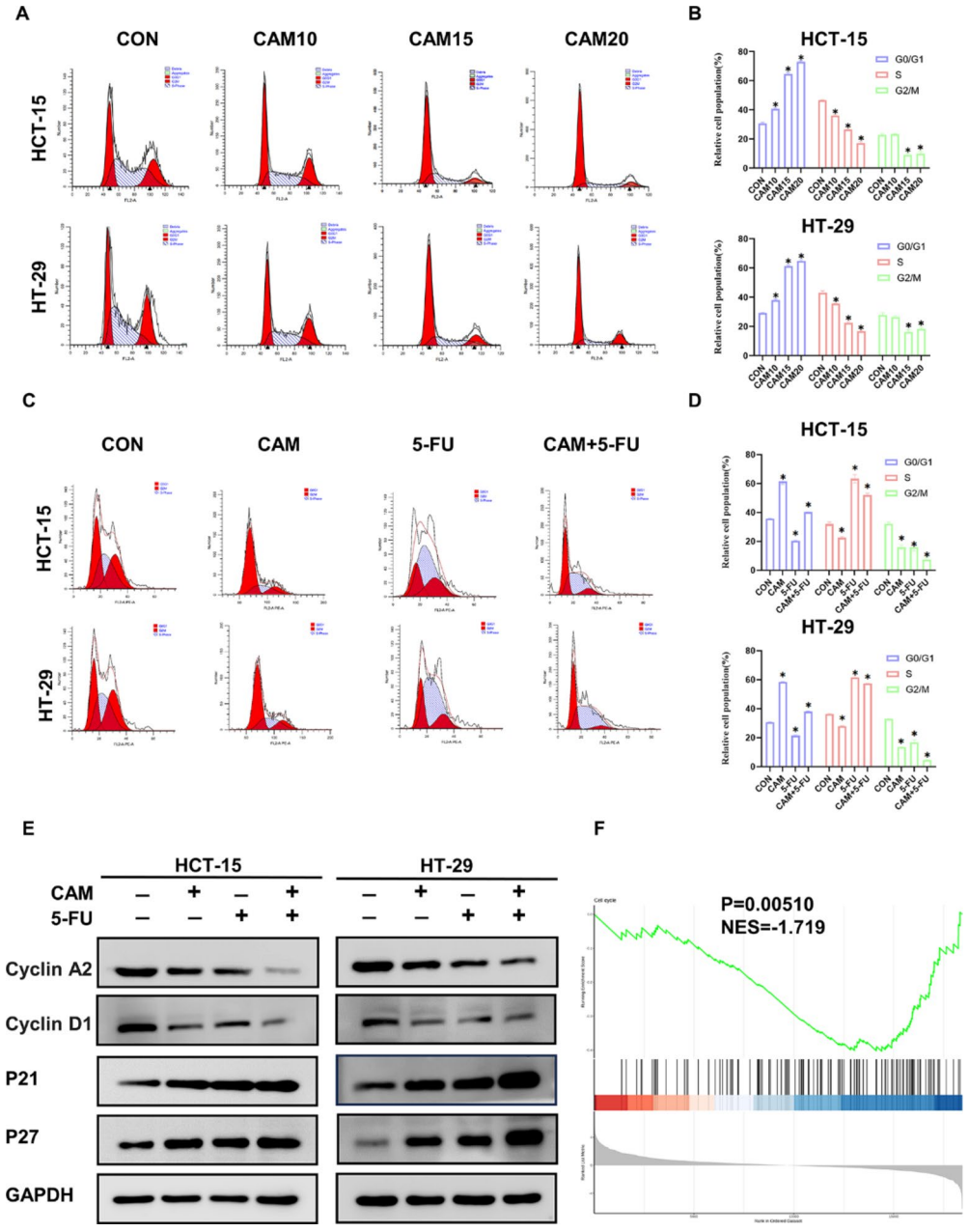

Fig. 3. Impact of CAM and 5-FU on Cell Cycle. (**A**-**B**) Cell cycle changes after CAM treatment. (**C**-**D**) Cell cycle changes after treatment with CAM, 5-FU, and CAM + 5-FU. (**E**) Western blot analysis of Cell cycle - related proteins, with GAPDH as a control. (**F**) Transcriptomics shows CAM + 5-FU activates the cell cycle pathway. Error bars indicate SEM. $^{*}P < 0.05$; $^{**}P < 0.01$; $^{***}P < 0.001$.

CAM and 5-FU treatment synergistically inhibits motility

To determine the effects of CAM and 5-FU on the horizontal and vertical migration abilities of CRC cells, we first performed a wound healing experiment. After 48 h, CAM + 5-FU showed a stronger inhibitory effect than either drug alone (Fig. 4A, B). Transwell migration assays further corroborated these findings, demonstrating that the CAM + 5-FU combination markedly reduced CRC cell migration (Fig. 4C, D). Moreover, an immunofluorescence analysis revealed that the combination treatment increased E-cadherin expression and reduced vimentin levels (Fig. 4E). The expression of proteins related to tumour metastasis, such as E-cadherin, vimentin, Snail, MMP-2, and MMP-9, was further evaluated to assess treatment efficacy. These results indicated that treatment with CAM + 5-FU was more effective than treatment with either drug alone (Fig. 4F), exhibiting a synergistic effect in reducing CRC cell migration.

CAM and 5-FU synergistically increase ROS levels

The fluorescent probe DCFH-DA was used to determine the intracellular ROS levels in CRC cells. The CAM group showed higher ROS levels than the control group. The CAM + 5-FU group exhibited the highest levels among all groups (Fig. 5A, B). To assess whether CAM combined with 5-FU inhibit CRC cell growth by

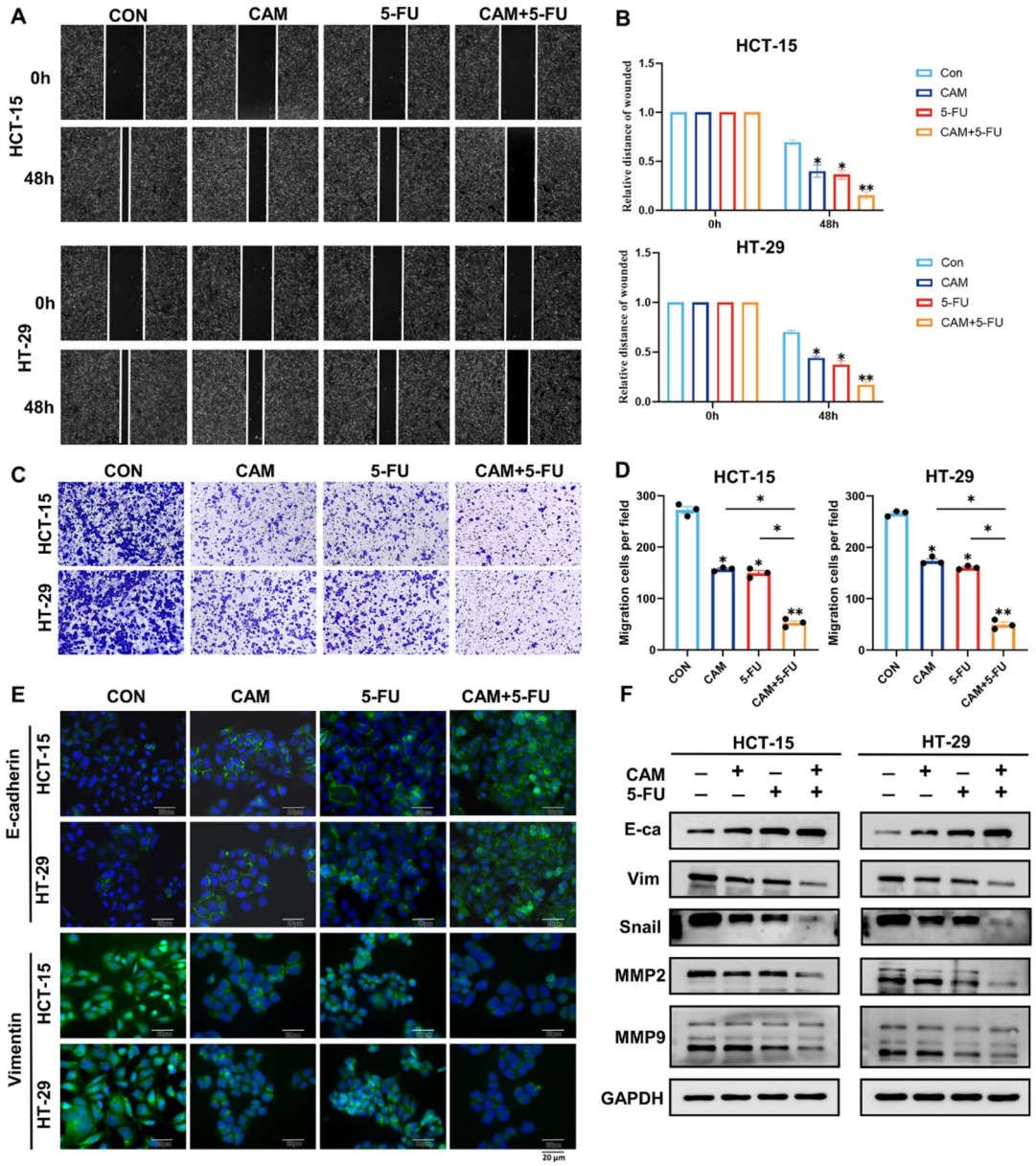

Fig. 4. CAM and 5-FU reduce CRC cell migration. (**A-D**) Wound healing and Transwell assays demonstrated decreased horizontal and vertical migration. (**E**) Immunofluorescence revealed EMT marker expression; scale bar: 20 μm. (**F**) Western blot confirmed EMT markers, with GAPDH as a control. $^{*}P < 0.05$; $^{**}P < 0.01$; $^{***}P < 0.001$. EMT, Epithelial-mesenchymal transition; E-ca, E-cadherin; Vim, vimentin.

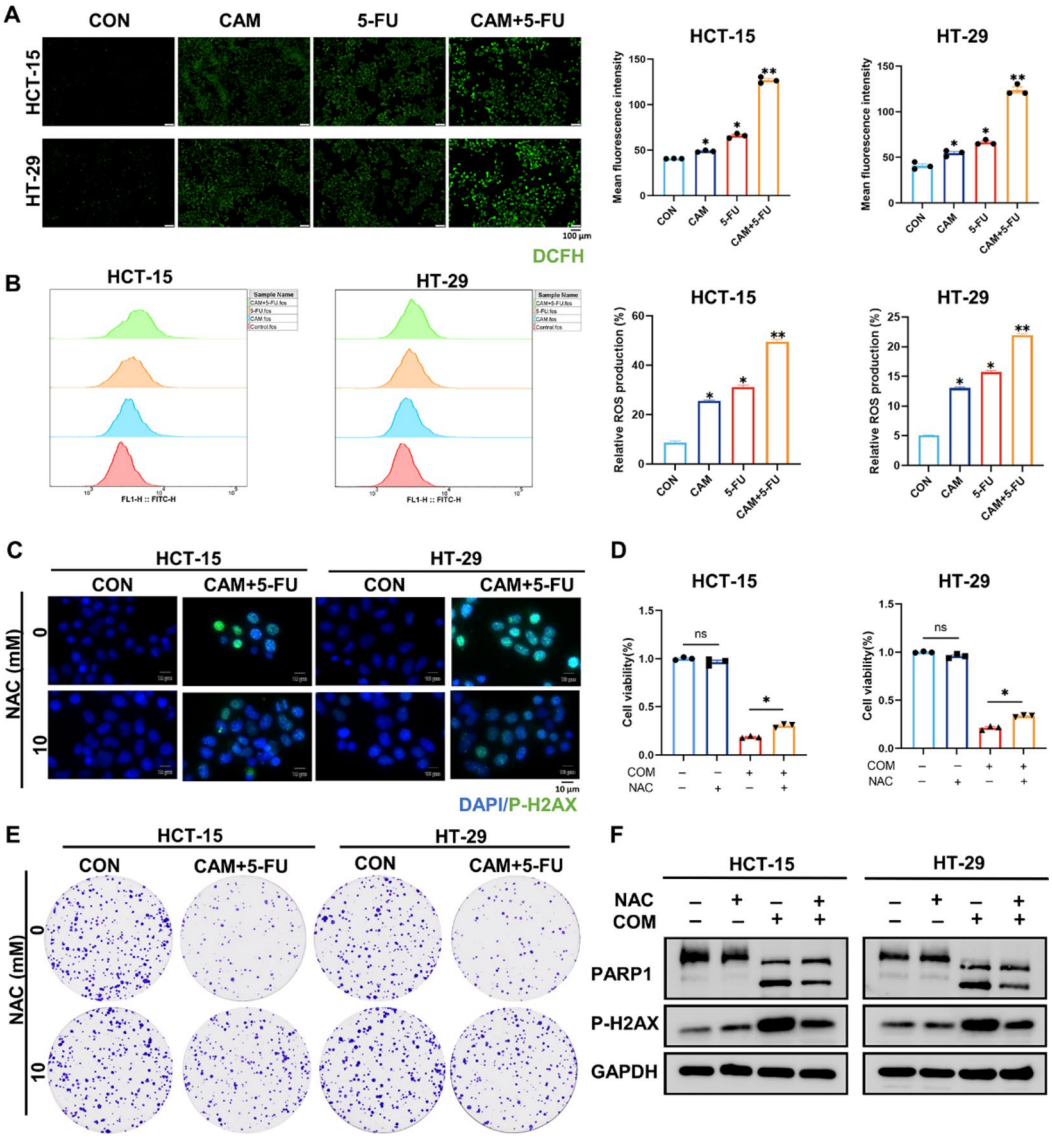

Fig. 5. The accumulation of ROS production induced by combination of CAM plus 5-FU. (**A**-**B**) ROS levels measured by (DCFH-DA). (**C**). Immunofluorescence to detect DNA damage levels. Scale bar, 10 μm. (**D**) CCK8 assay for cell viability. (**E**) Colony formation analysis. (**F**) Western blot analysis PARP1 and P-H2AX protein. *$P < 0.05$; **$P < 0.01$; ***$P < 0.001$. COM, combination.

increasing ROS levels, CRC cells were treated with or without 10 mM N-acetylcysteine (NAC), an antioxidant. NAC treatment decreased DNA damage, restored cell viability and clonogenicity, and reversed c-PARP and P-H2AX expression (Fig. 5C–F and supplementary Fig. S1C). These results indicated that CAM + 5-FU may increase ROS levels and cause DNA damage.

RNA-seq analysis supports the regulation of the MAPK pathway

A total of 2896 differentially expressed genes (DEGs) were identified between the CON and CAM + 5-FU groups using RNA-seq analysis (fold change > 1.5 and false discovery rate < 0.05). Among these genes, 1509 were upregulated, and 1387 were downregulated (Fig. 6A, B). Kyoto Encyclopedia of Genes and Genomes (KEGG) pathway analyses of these DEGs indicated significant enrichment in MAPK pathways (Fig. 6C, D), suggesting that these pathways play a pivotal role in cell death induced by CAM and 5-FU. As many anticancer agents trigger ROS and activate the MAPK pathway, leading to apoptosis, the JNK/p38 MAPK proteins were further explored. Western blot analysis indicated that CRC cells treated with CAM, 5-FU, or their combination exhibited significantly increased p38, JNK, and c-Jun phosphorylation (Fig. 6E). Our results suggested that CAM enhanced the tumour-suppressive effect of 5-FU, possibly through activating the JNK/p38 signalling pathway, thereby interfering with CRC cell survival.

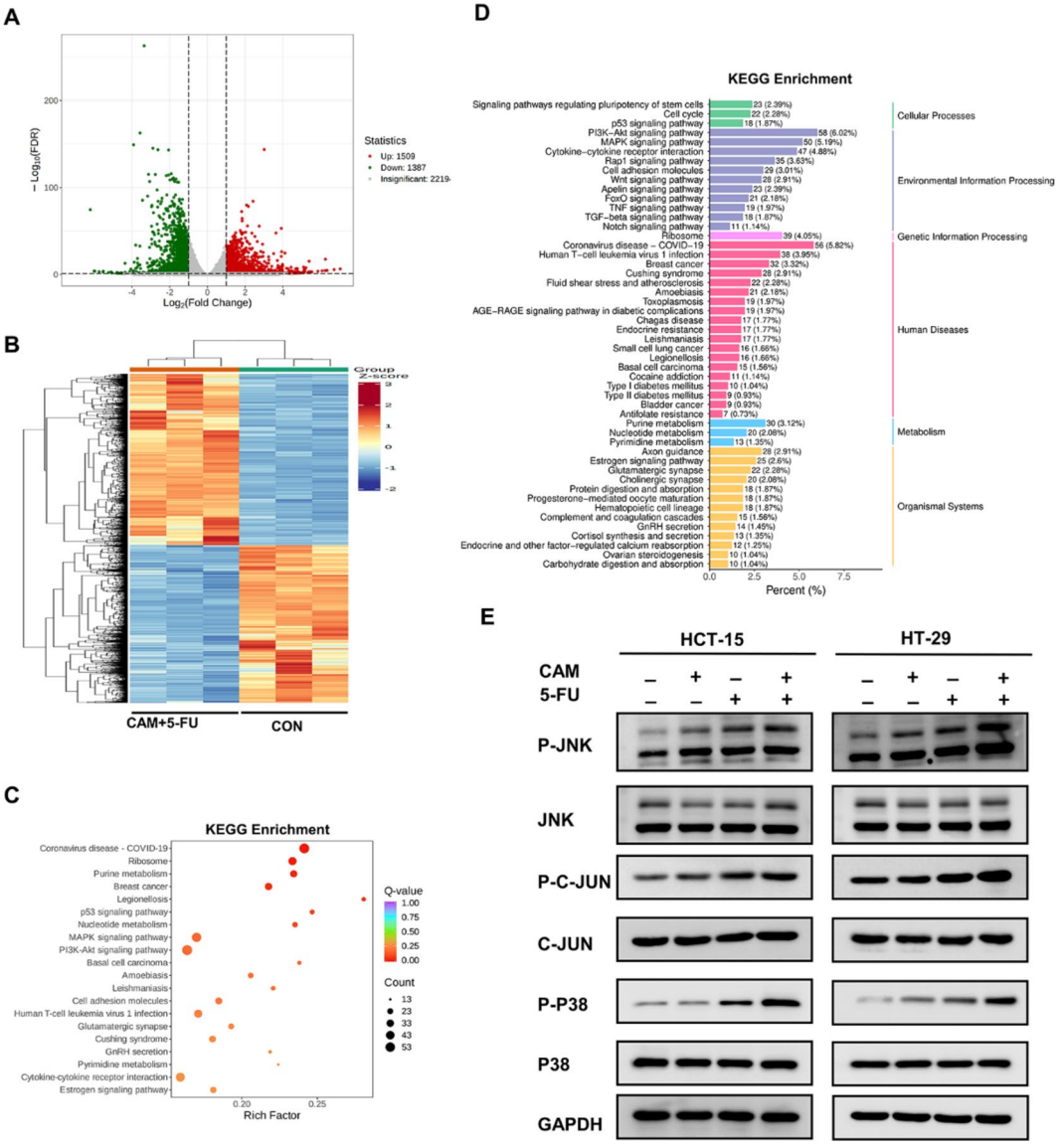

Fig. 6. RNA-seq analysis showed CAM and 5-FU cotreatment enriched the MAPK pathway. (**A**) Volcano plot of dysregulated genes between CON and CAM + 5-FU groups. (**B**) Heatmap of differentially expressed genes in CAM + 5-FU vs. CON groups. (**C**) KEGG enrichment histograms of differential genes. (**D**) KEGG enrichment scatter plot. (E) MAPK pathway protein expression levels, with GAPDH as a control. Error bars show SEM. $^{*}P < 0.05$; $^{**}P < 0.01$; $^{***}P < 0.001$.

CAM combined with 5-FU enhanced the Inhibition of tumour growth in xenograft mouse models

To examine the combined effects of CAM and 5-FU, a subcutaneous tumour model was established in nude mice using HCT-15 cells (Fig. 7A). Representative tumour images are shown in Fig. 7B. The combination treatment significantly reduced tumour mass (Fig. 7D) and tumour volume compared with those in the PBS, 5-FU, and CAM groups (Fig. 7E). Importantly, neither CAM nor 5-FU alone, nor the CAM + 5-FU combination caused weight loss, indicating the absence of systemic toxicity (Fig. 7F). TUNEL staining revealed that the tumour apoptosis rate was highest in the CAM + 5-FU group. Immunohistochemical (IHC) staining demonstrated a significant downregulation of Ki-67 in the CAM + 5-FU group, highlighting the potential of CAM to inhibit tumour growth. Moreover, no systemic toxicity was observed in the liver and kidney sections under a light microscope (Fig. 7C). Overall, these results demonstrated the safety of the CAM + 5-FU combination treatment, which synergistically inhibited tumour growth in vivo.

Discussion

Macrolide antitumour antibiotics inhibit ribosome biogenesis, show significant anticancer potential by inhibiting cell proliferation, and are more specific than most chemotherapeutic agents, leading to improved efficacy and fewer side effects[24]. CAM exhibited significant chemosensitisation by augmenting the inhibitory effects of 5-FU

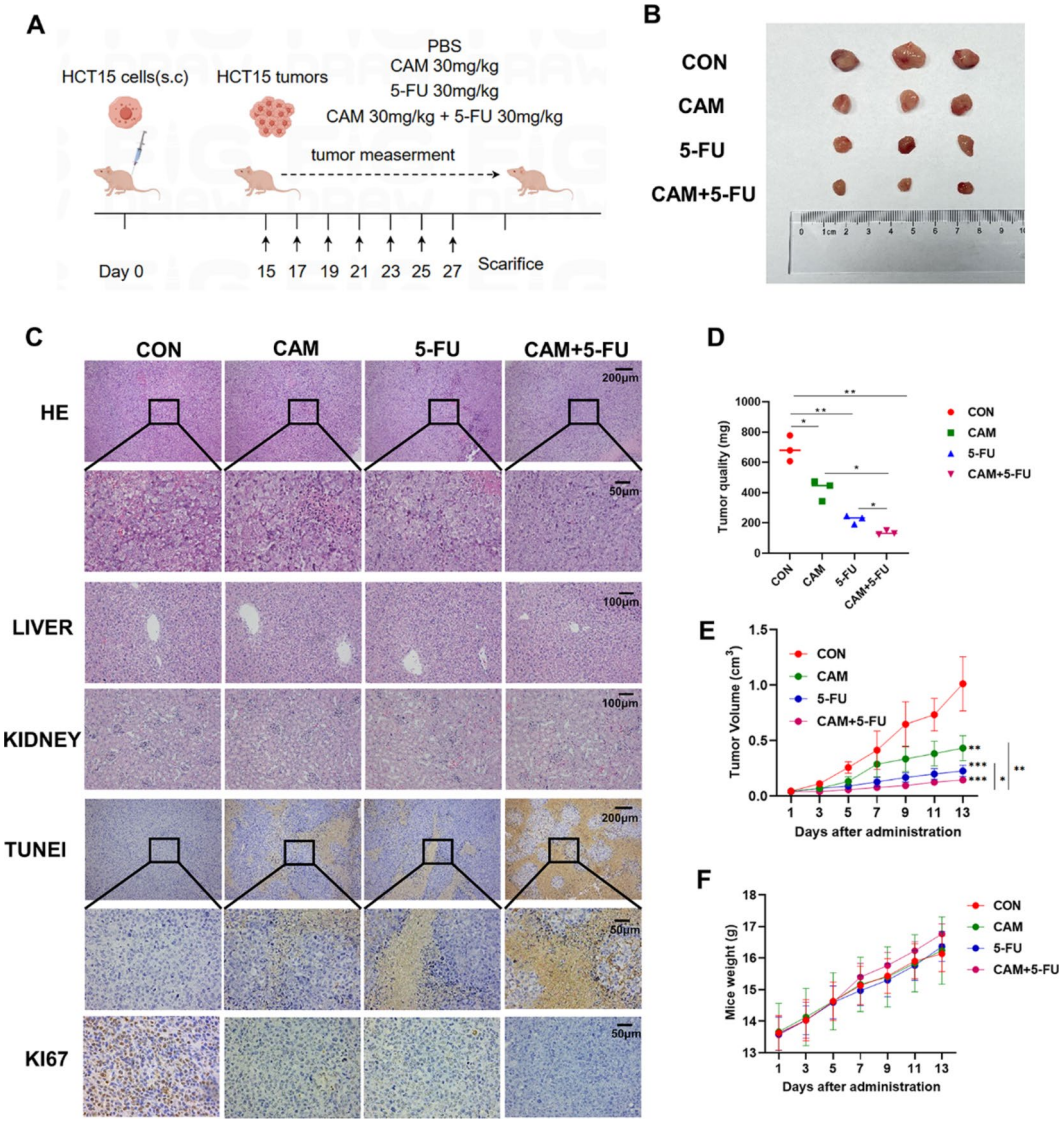

Fig. 7. CAM combined with 5-FU more effectively inhibited tumour growth in *vivo*. (**A**) Treatment plan for tumour-bearing mice. (**B**) Photos of excised tumours. (**C**) HE staining, TUNEL analysis, and Ki67 immunohistochemistry of tumour tissue. Tumour weight (**D**), volume (**E**), and mouse weight (**F**) across groups. Error bars show SEM. $^{*}P<0.05$; $^{**}P<0.01$; $^{***}P<0.001$.

on CRC cell proliferation and reducing the necessary dose of 5-FU to achieve the desired therapeutic outcome, thereby mitigating the resistance and negative effects associated with increased doses. These findings indicated that the combination of CAM and 5-FU could be an effective clinical treatment approach. The mechanisms underlying the systemic antitumor effects of CAM and 5-FU are shown in Fig. 8.

CAM, as a therapeutic sensitiser, has shown excellent effects in promoting apoptosis. Jin and Liang showed that CAM has good cytotoxicity in hepatocellular carcinoma and oral squamous cell carcinoma cells[25,26]. Our results showed that the combination of CAM and 5-FU was more effective in inducing apoptosis, and that CAM could increase the cytotoxic synergy of 5-FU by increasing the rate of apoptosis. Furthermore, TUNEL staining analysis showed that the highest apoptosis rate was observed with the combination of CAM and 5-FU. PARP1 degradation is an important indicator of programmed cell death[27]. An imbalance in the levels of Bax and Bcl-2 results in the release of cytochrome C from the mitochondria[28]. Mitochondrial cytochrome C release enables Apaf1 aggregation and, with Bcl-2 family proteins such as Bax-forming channels, triggers sustained caspase activation, leading to apoptosis[29]. Furthermore, we observed that 89-kDa PARP1, Bax/Bcl-2, and CYC1 were significantly upregulated after CAM and 5-FU treatment, suggesting that CAM and 5-FU induced cell death in CRC cells via the mitochondrial route.

Drugs causing DNA damage are increasingly being developed as antitumour treatments. The anti-tumour effect of 5-FU involves its conversion to FdUMP and subsequently to FdUTP, which can replace dTTP during DNA replication, leading to the incorporation of 5-FU-containing nucleotides that disrupt the normal DNA structure and function[30,31]. Consequently, 5-FU induces cytotoxic effects by disrupting DNA replication,

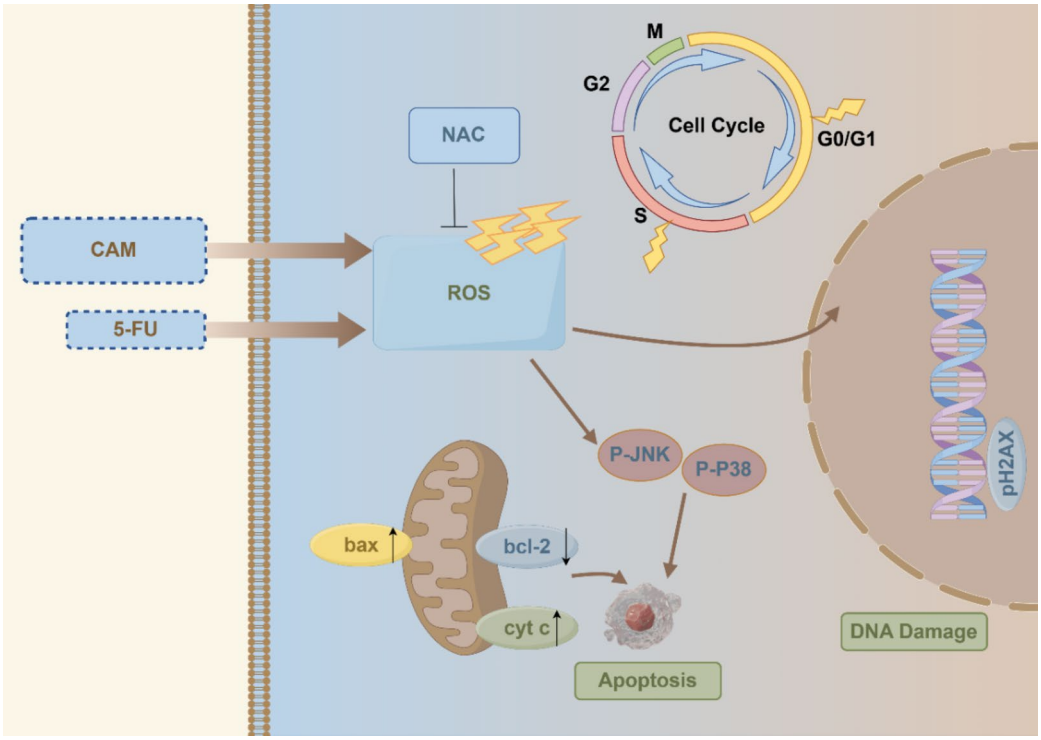

Fig. 8. Mechanism of tumour suppression by CAM combined with 5-FU.

preventing cell cycle progression, and initiating apoptosis[31,32]. P-H2AX is one of the early hallmarks of DNA double-strand breaks and can recruit repair proteins to the damage site, thereby initiating the repair process[33]. Our results demonstrated that CAM inhibited cell proliferation by enhancing 5-FU-induced DNA damage. Similarly, Xu showed that isovalerylspiramycin I inhibits the growth of small-cell lung cancer cells via the ATR/CHK1 pathway in response to DNA damage[14]. In the presence of DNA damage, the DNA damage sensor ATM/ATR is recruited to DNA double-strand breaks, ATM/ATR phosphorylates downstream CHK1/2, and Chk2 inhibits CDC25A activation; CDC25A-mediated activation of CDK2/4/6 promotes the transition of the cell cycle from the G1 phase to the S phase. After the inhibition of CDC25A activity, the cell cycle is stalled in the G1/S or G2/M phase; thus, DNA damage signals cell cycle arrest[34]. Our results indicated that CAM induced a significant cell cycle blockade and enhanced DNA damage.

ROS mediate the induction of nucleolar DNA damage, cell cycle arrest, and apoptosis caused by various anticancer drugs[35–37]. ROS can oxidise cardiolipin, causing mitochondrial membrane depolarisation and release of cytochrome C into the cytosol[38]. Cytochrome C creates apoptotic vesicles that trigger effector caspases, causing protein fragmentation, and DNA damage, and ultimately apoptosis[36]. For example, Zhang showed that sodium selenite increased ROS levels in breast cancer cells, resulting in mitochondrial dysfunction and subsequent caspase activation, which initiated the mitochondria-induced apoptosis pathway[39]; Liu showed that CAM can be used as a novel ROS inducer to inhibit the growth of non-small cell lung cancer[13]; and Cui demonstrated that ISP I specifically inhibits selenoprotein H and enhances intracellular ROS production in glioblastoma cells[11]. Based on these findings, we investigated the role of CAM in CRC treatment by modulating ROS levels. Our findings indicated that combination therapy with CAM and 5-FU increased ROS levels in CRC, and the inhibition of ROS production led to decreased expression of P-H2AX and cleaved PARP1, ultimately reviving cell viability and proliferation. Hence, our results suggests that CAM and 5-FU induce DNA damage and apoptosis through ROS generation, thereby providing a new direction for future studies.

Targeting JNK and p38 MAPK is a promising approach, as their activation is crucial in drug-induced apoptosis[40]; moreover, studies have shown that p38 and JNK can be activated by ROS to induce apoptosis[41,42]. The activation of JNK may trigger antioxidant responses that lead to cell death[43]. JNK activates AP-1 by phosphorylating c-Jun, promoting Fas/FasL pathway proteins to induce apoptosis. JNK also phosphorylates Bcl-2/Bcl-xL, disrupting the mitochondrial membrane potential and releasing cytochrome C to trigger apoptosis[44]. Additionally, increasing evidence suggests that p38 acts as an oncogene by activating the p38 MAPK to enhance chemotherapy-induced apoptosis[45]. Pang reported that cyclophosphamide initiates apoptosis in breast cancer cells by activating p38 [17], and anthocyanins from herbs promote apoptosis by activating p38 in CRC cells[46]. In line with these findings, our study showed that CAM and 5-FU increased JNK/p38 MAPK phosphorylation and upregulated c-Jun phosphorylation in CRC cells.

The current application of CAM for the clinical treatment of CRC faces some challenges. Conducting widespread clinical trials is a vital step in confirming its safety and efficacy because in the clinical setting, various

factors, such as individual patient differences, tumour heterogeneity, and drug combinations, can affect the final effect of the drug. However, appropriate drug dosages, regimens, and combination regimens must be determined.

Materials and methods

Cell culture and reagents

The Key Laboratory of Pathobiology at Yanbian University provided human CRC cells (HCT-15, HT-29), which were maintained in RPMI 1640 medium supplemented with 10% FBS (Gibco), and utilised within 20 passages. CAM was provided by the Key Laboratory of Pathobiology (Yanbian University), and 5-FU and NAC were purchased from MCE.

Cell viability assay

A concentration of 2×10^3 cells was added to each well of the 96-well plates, and subjected to specific amounts of CAM (0, 2, 4, 8, 16, 32 μg/ml), or 5-FU (0, 10, 20, 40, 80, 160 μM) for 24 h. A 1:10 ratio of Cell Counting Kit-8 (CCK8) (Invigentech, California, USA) and 1640 medium was added and incubated in the dark for 4 h, and the absorbance was assessed at 450 nm. (TECAN, SARK, 10 M).

Assessment of the synergistic effect

Concentration gradients of CAM and 5-FU were pre-determined based on the IC_{50} values for each drug. Cell viability was analysed using a constant dilution ratio of the two drugs. After treatment with CAM at concentrations of 0, 6, 12, and 18 μg/mL and 5-FU at 0, 17.5, 35, and 52.5 μM for 48 h, cell viability was detected using the CCK-8 reagent as described above. The analysis was performed using the online SynergyFinder software (https://synergyfinder.fimm.fi). The drug synergy score with inhibition index (inhibition index = 100-cell viability) was calculated using the HSA calculation method. An HSA synergy score of less than 10 indicates that the interaction between the two drugs is likely to be antagonistic; from − 10 to 10, the interaction between the two drugs may be additive; and greater than 10, the interaction between the two drugs is likely to be synergistic. The grades in the red area indicate the strength of the synergistic effect[47].

FITC-Annexin V/PI staining assay

Cells were incubated with CAM, 5-FU, and CAM + 5-FU for 24 h, The cells were digested with trypsin without EDTA, carefully collected into centrifuge tubes, and then centrifuged at 1000 rpm for 5 min. The supernatant was discarded, the cells were resuspended in PBS, and then counted. In each group, 5×10^5 cells were mixed with 500 μL of 1× binding buffer. FITC-Annexin V (5 μl) and PI dye (10 μl) (Annexin V-FITC kit, Beyotime) were added for 10 min. The prepared mixture was subjected to flow cytometry.

IF staining

The cells were cultured on slides until they reached the required density, fixed with 4% paraformaldehyde, permeabilised with Triton X-100, and blocked with BSA. The cells were then exposed to a primary antibody that bound to the target protein, followed by incubation with an FITC-labelled secondary antibody. To protect the fluorescent signal, the slides were stored in the dark. Nuclear staining was performed using DAPI, and fluorescence microscopy was used to capture images of the cells.

Western blot

The cells were lysed using PIPA buffer (Beyotime, Shanghai, China) containing protease and phosphatase inhibitors. Coomassie Brilliant Blue method was used for protein quantification. Proteins were denatured and separated using sodium dodecyl sulfate-polyacrylamide gel electrophoresis. The membrane was blocked using non-fat powdered milk, followed by incubation with a primary antibody (PARP1 (13371-1-AP), CYC1 (10242-1-AP), P-H2AX (29380-1-AP), Bax (50599-2-IG), Bcl-2 (12789-1-AP), MMP2 (10373-2-AP), MMP9 (10375-2-AP), P21 (10355-1-AP), E-cadherin (20874-1-AP), Vimentin (10366-1-AP), Snail (12129-1-AP), JNK (24164-1-AP), P-JNK (80024-1-RR), C-JUN (24909-1-AP), P-C-JUN (28891-1-AP), p38 MAPK (14064-1-AP), phospho-p38 MAPK (28796-1-AP), Cyclin D1(26939-1-AP), Cyclin A2(18202-1-1P), P27 (610242)) targeting the protein. The secondary antibody GAPDH (10494-1-AP) was bound to the primary antibody. Chemiluminescence revealed protein bands, which were imaged to assess the presence and quantity of proteins.

Cell cycle

We applied CAM, 5-FU, and CAM + 5-FU to the cells for 48 h. Afterwards, the cells were digested for cell suspension. The suspension was centrifuged for cell counting, and 1×10^6 cells were collected for each group, fixed in 70% ethanol at −20 °C for 24 h, cleaned with PBS, and incubated with RNase A and PI for 30 min. Flow cytometry was then performed using the Cell Quest software (Becton Dickinson).

Wound-healing assay

A six-well plate was seeded at a density of 1×10^6cells per well. After the cells attached to the substrate, a pipette tip was used to scratch them. The medium was then replaced, and specified amounts of CAM, 5-FU, and CAM + 5-FU were added. After 48 h, the medium was replaced with fresh medium. Images of cell migration were collected at 0 and 48 h using a light microscope (OLYMPUS IX73). ImageJ software was used to calculate the wound area and determine the cell migration ratio[48].

Transwell

The cells were digested and centrifuged to prepare single-cell suspensions. The Transwell chamber was placed in a 24-well plate. Then, 100 μL of the cell suspension with 3×10^5cells per well was added to the upper chamber.

Subsequently, 800 µL of the culture medium containing serum was added to the lower chamber. The plates were incubated for 24 h. The cells were then fixed with formaldehyde for 20 min, washed with PBS, stained with crystal violet for 30 min, and finally washed three times with PBS. Images were captured under a microscope, and the cells were counted using ImageJ[48].

Total ROS assay

After treating the cells with CAM, 5-FU, and CAM + 5-FU for 24 h, they were incubated with 5 mM DCFH-DA probe at 37 °C for 30 min. Subsequently, the cells were washed thrice with serum-free medium. The fluorescence distribution was then detected separately using fluorescence microscopy and flow cytometry.

Colony formation assay

In the six-well plates, cells were seeded at a density of 1,500 per well; treated with CAM, 5-FU, and CAM + 5-FU for 48 h; and then cultured in fresh medium for two weeks. Subsequently, the cells were fixed, stained with crystal violet, air-dried, and then imaged.

RNA sequence and KEGG annotation

CRC cells were treated with CAM + 5-FU for 48 h. TRIzol reagent was added to extract RNA. High-throughput RNA sequencing was performed using the Illumina platform. Analyze the differential gene expression between the treatment and the control using the DESeq R software package[49]. KEGG enrichment[50,51] were used for visualization processing with R software.

In vivo CRC xenograft model

Animal experiments were approved by the ethics committee of Yanbian University (program No. YD20241014007). Twelve 4–6-week-old SPF BALB/c male nude mice were obtained from the Beijing Vital River Laboratory and housed at the Experimental Animal Centre in Yanbian University. After one week of acclimatisation, each mouse was subcutaneously injected with 5×10^6 HCT-15 cells. When the tumours measured 100 mm^3, the mice were randomly assigned to four groups: PBS, CAM, 5-FU, and CAM + 5-FU groups. Subsequently, PBS (control), CAM (30 mg/kg), 5-FU (30 mg/kg), and CAM + 5-FU (30 mg/kg each) were administered intraperitoneally every two days. Additionally, the body weights of the mice were monitored. Tumour Volume (mm3) = (length) × $(\text{width})^2 \times 0.5$. After seven administrations of the drug, the mice were euthanised by injecting sodium pentobarbital.

Haematoxylin-eosin (HE) staining

After seven treatments, the mice were sacrificed, and the tumours were collected. Liver and kidney tissues were collected to evaluate systemic toxicity and treated with 4% paraformaldehyde for 48 h. Specimens were embedded in paraffin and sectioned into slices measuring 4–5 µm. Sections were stained with haematoxylin and eosin according to a standard protocol and examined under a light microscope.

TUNEL staining

The TUNEL assay was used to assess apoptosis in mouse CRC samples. Initially, tissue sections were dewaxed and hydrated. Subsequently, they were treated with Proteinase K to enhance permeability. Next, the TUNEL reaction mixture was added, and the sections were incubated at 37 °C in the dark for 60 min. A DAB chromogenic reaction was then carried out, staining the apoptotic cell nuclei brown, whereas haematoxylin was used to stain the nuclei blue. Finally, the samples were examined under an optical microscope.

Immunohistochemical (IHC) staining

For IHC staining, ethylenediaminetetraacetic acid (EDTA) buffer (pH 8.0) was used to treat sections for antigen repair and then blocked with 3% H2O2. The primary antibody Ki-67 (1:200, 27309-1-AP) was used overnight at a temperature of 4 °C and then incubated for two hours with a secondary antibody that is HRP-conjugated (1:100). The DAB substrate was used, followed by haematoxylin nuclear counterstaining, alcohol dehydration, and xylene hyaluronidation, with brown granules indicating positive staining.

Ethynyl-2′-deoxyuridine (EdU) assay

Cells were treated with defined amounts of CAM, 5-FU, and CAM + 5-FU; then, an EdU solution (50 µM; 100 µl per well) was added and incubated for 2 h. Afterwards, cells were treated with 4% paraformaldehyde (50 µl per well) for 30 min, followed by glycine (2 mg/ml; 50 µl per well) for 5 min, and then 0.5% Triton X-100 (100 µl per well) for 10 min. Each well received 100 µl of 1× Apollo staining solution for 30 min, then placed in the dark with 0.5% Triton X-100 (100 µl per well). Cells were imaged using a fluorescence microscope (OLYMPUS IX73), followed by analysis using the ImageJ software[48].

Statistical analysis

The research results were statistically analysed using GraphPad Prism 9.0 and the online SynergyFinder software. Data are presented as mean ± SEM. One-way ANOVAs were used for statistical analysis. $^*P < 0.05$; $^{**}P < 0.01$; $^{***}P < 0.001$.

Data availability

The datasets generated and/or analysed during the current study are available in the NCBI repository, relevant accession numbers: PRJNA1229789.

Received: 13 January 2025; Accepted: 12 March 2025
Published online: 17 March 2025

References

1. Siegel, R. L., Giaquinto, A. N. & Jemal, A. Cancer statistics, 2024. *CA Cancer J. Clin.* **74**, 12–49 (2024).
2. Biller, L. H. & Schrag, D. Diagnosis and treatment of metastatic colorectal cancer: A review. *JAMA* **325**, 669–685 (2021).
3. Sethy, C. & Kundu, C. N. 5-Fluorouracil (5-FU) resistance and the new strategy to enhance the sensitivity against cancer: implication of DNA repair Inhibition. *Biomed. Pharmacother.* **137**, 111285 (2021).
4. Conroy, T. et al. Neoadjuvant chemotherapy with FOLFIRINOX and preoperative chemoradiotherapy for patients with locally advanced rectal cancer (UNICANCER-PRODIGE 23): a multicentre, randomised, open-label, phase 3 trial. *Lancet Oncol.* **22**, 702–715 (2021).
5. Abedizadeh, R., Majidi, F., Khorasani, H. R., Abedi, H. & Sabour, D. Colorectal cancer: a comprehensive review of carcinogenesis, diagnosis, and novel strategies for classified treatments. *Cancer Metastasis Rev.* **43**, 729–753 (2024).
6. Dinos, G. P. The macrolide antibiotic renaissance. *Br. J. Pharmacol.* **174**, 2967–2983 (2017).
7. Li, H. et al. Carrimycin inhibits coronavirus replication by decreasing the efficiency of programmed – 1 ribosomal frameshifting through directly binding to the RNA pseudoknot of viral frameshift-stimulatory element. *Acta Pharm. Sin B.* **14**, 2567–2580 (2024).
8. Nan, C. et al. Effects of Carrimycin on biomarkers of inflammation and immune function in tumor patients with sepsis: A multicenter double-blind randomized controlled trial. *Pharmacol. Res.* **198**, 106991 (2023).
9. Hanahan, D. Hallmarks of cancer: new dimensions. *Cancer Discov.* **12**, 31–46 (2022).
10. Du, N. et al. Carrimycin, as one of the drugs in combination therapy, for the treatment of Carbapenem-Resistant acinetobacter baumannii infection. *Infect. Drug Resist.* **17**, 3617–3621 (2024).
11. Cui, J. et al. Targeting Selenoprotein H in the nucleolus suppresses tumors and metastases by isovalerylspiramycin I. *J. Exp. Clin. Cancer Res.* **41**, 126 (2022).
12. Sy, L. et al. Anti-tumor effect of carrimycin on oral squamous cell carcinoma cells in vitro and in vivo. *Translational Oncol.* **14**, 101074 (2021).
13. Liu, Z. et al. Isovalerylspiramycin I suppresses non-small cell lung carcinoma growth through ROS-mediated Inhibition of PI3K/AKT signaling pathway. *Int. J. Biol. Sci.* **18**, 3714–3730 (2022).
14. Xu, Y. Isovalerylspiramycin I suppresses small cell lung cancer proliferation via ATR/CHK1 mediated DNA damage response and PERK/eIF2α/ATF4/CHOP mediated ER stress. *Biochem. Pharmacol.* https://doi.org/10.1016/j.bcp.2024.116557 (2024).
15. GUANGDONG, S., JIANLU, D. & YIGUANG, W. Construction and physiological studies on a stable bioengineered strain of Shengjimycin. *J. Antibiot.* **54**, 66–73 (2001).
16. Wagner, E. F. & Nebreda, Á. R. Signal integration by JNK and p38 MAPK pathways in cancer development. *Nat. Rev. Cancer.* **9**, 537–549 (2009).
17. Pang, H. et al. Knockdown of osteopontin chemosensitizes MDA-MB-231 cells to cyclophosphamide by enhancing apoptosis through activating p38 MAPK pathway. *Cancer Biother Radiopharm.* **26**, 165–173 (2011).
18. Chiu, S. J., Chao, J. I., Lee, Y. J. & Hsu, T. S. Regulation of gamma-H2AX and securin contribute to apoptosis by oxaliplatin via a p38 mitogen-activated protein kinase-dependent pathway in human colorectal cancer cells. *Toxicol. Lett.* **179**, 63–70 (2008).
19. Mansouri, A. et al. Sustained activation of JNK/p38 MAPK pathways in response to cisplatin leads to Fas ligand induction and cell death in ovarian carcinoma cells. *J. Biol. Chem.* **278**, 19245–19256 (2003).
20. Kwak, A. W. et al. Echinatin induces reactive oxygen species-mediated apoptosis via JNK/p38 MAPK signaling pathway in colorectal cancer cells. *Phytother Res.* **37**, 563–577 (2023).
21. Kwak, A. W. et al. Isolinderalactone sensitizes oxaliplatin-resistance colorectal cancer cells through JNK/p38 MAPK signaling pathways. *Phytomedicine* **105**, 154383 (2022).
22. Seo, S. Y. et al. Activation of p38 and JNK by ROS contributes to Deoxybouvardin-Mediated intrinsic apoptosis in Oxaliplatin-Sensitive and -Resistant colorectal cancer cells. *Antioxid. (Basel).* **13**, 866 (2024).
23. Yu, M., Chen, Q. & Lu, Y. P. Aldehyde dehydrogenase 2 family member repression promotes colorectal cancer progression by JNK/p38 MAPK pathways-mediated apoptosis and DNA damage. *World J. Gastrointest. Oncol.* **16**, 3230–3240 (2024).
24. Burger, K. et al. Chemotherapeutic drugs inhibit ribosome biogenesis at various levels. *J. Biol. Chem.* **285**, 12416–12425 (2010).
25. Liang, S. et al. Anti-tumor effect of Carrimycin on oral squamous cell carcinoma cells in vitro and in vivo. *Transl Oncol.* **14**, 101074 (2021).
26. Jin, Y. et al. Anti-Tumor effects of Carrimycin and monomeric isovalerylspiramycin I on hepatocellular carcinoma in vitro and in vivo. *Front. Pharmacol.* **12**, 774231 (2021).
27. Whitacre, C. M., Zborowska, E., Willson, J. K. & Berger, N. A. Detection of poly(ADP-ribose) polymerase cleavage in response to treatment with topoisomerase I inhibitors: a potential surrogate end point to assess treatment effectiveness. *Clin. Cancer Res.* **5**, 665–672 (1999).
28. Pagliara, V. et al. 5-FU targets rpL3 to induce mitochondrial apoptosis via cystathionine-β-synthase in colon cancer cells lacking p53. *Oncotarget* **7**, 50333–50348 (2016).
29. Zhao, Q. et al. GLUD1 inhibits hepatocellular carcinoma progression via ROS-mediated p38/JNK MAPK pathway activation and mitochondrial apoptosis. *Discov Oncol.* **15**, 8 (2024).
30. Mori, R. et al. The Inhibition of thymidine phosphorylase can reverse acquired 5FU-resistance in gastric cancer cells. *Gastric Cancer.* **22**, 497–505 (2019).
31. Longley, D. B., Harkin, D. P. & Johnston, P. G. 5-fluorouracil: mechanisms of action and clinical strategies. *Nat. Rev. Cancer.* **3**, 330–338 (2003).
32. Johnson, K. R., Wang, L., Miller, M. C., Willingham, M. C. & Fan, W. 5-Fluorouracil interferes with Paclitaxel cytotoxicity against human solid tumor cells. *Clin. Cancer Res.* **3**, 1739–1745 (1997).
33. Prabhu, K. S. et al. H2AX: A key player in DNA damage response and a promising target for cancer therapy. *Biomed. Pharmacother.* **175**, 116663 (2024).
34. Zgheib, O. et al. ATM signaling and 53BP1. *Radiother Oncol.* **76**, 119–122 (2005).
35. Yu, L. C. et al. Carrimycin, a first in-class anti-cancer agent, targets Selenoprotein H to induce nucleolar oxidative stress and inhibit ribosome biogenesis. *Cancer Pathog Ther.* **1**, 111–115 (2023).
36. Srinivas, U. S., Tan, B. W. Q., Vellayappan, B. A. & Jeyasekharan, A. D. ROS and the DNA damage response in cancer. *Redox Biol.* **25**, 101084 (2019).
37. Tudek, B. et al. Involvement of oxidatively damaged DNA and repair in cancer development and aging. *Am. J. Transl Res.* **2**, 254–284 (2010).
38. Chaudhry, G. E. S., Akim, M., Sung, A., Sifzizul, T. M. T. & Y. Y. & Cancer and apoptosis: the apoptotic activity of plant and marine natural products and their potential as targeted cancer therapeutics. *Front. Pharmacol.* **13**, 842376 (2022).
39. Zhang, T. et al. Sodium selenite induces apoptosis via ROS-mediated NF-κB signaling and activation of the Bax-caspase-9-caspase-3 axis in 4T1 cells. *J. Cell. Physiol.* **234**, 2511–2522 (2019).
40. Circu, M. L. & Aw, T. Y. Reactive oxygen species, cellular redox systems, and apoptosis. *Free Radic Biol. Med.* **48**, 749–762 (2010).
41. Perillo, B. et al. ROS in cancer therapy: the bright side of the Moon. *Exp. Mol. Med.* **52**, 192–203 (2020).

42. Dolado, I. et al. p38α MAP kinase as a sensor of reactive oxygen species in tumorigenesis. *Cancer Cell.* **11**, 191–205 (2007).
43. Li, Y. et al. JNK-dependent Atg4 upregulation mediates asperphenamate derivative BBP-induced autophagy in MCF-7 cells. *Toxicol. Appl. Pharmacol.* **263**, 21–31 (2012).
44. Sui, X. et al. p38 and JNK MAPK pathways control the balance of apoptosis and autophagy in response to chemotherapeutic agents. *Cancer Lett.* **344**, 174–179 (2014).
45. Deacon, K., Mistry, P., Chernoff, J., Blank, J. L. & Patel, R. p38 Mitogen-activated protein kinase mediates cell death and p21-activated kinase mediates cell survival during chemotherapeutic drug-induced mitotic arrest. *Mol. Biol. Cell.* **14**, 2071–2087 (2003).
46. Dy, S. et al. Induction of apoptosis in human colon cancer HCT-116 cells by anthocyanins through suppression of Akt and activation of p38-MAPK. *Int. J. Oncol.* **35**, 1499–1504 (2009).
47. Zheng, S. et al. SynergyFinder plus: toward better interpretation and annotation of drug combination screening datasets. *Genomics Proteom. Bioinf.* **20**, 587–596 (2022).
48. Grishagin, I. V. Automatic cell counting with ImageJ. *Anal. Biochem.* **473**, 63–65 (2015).
49. Varet, H., Brillet-Guéguen, L., Coppée, J. Y., Dillies, M. A. & SARTools A DESeq2- and EdgeR-Based R pipeline for comprehensive differential analysis of RNA-Seq data. *PLoS One.* **11**, e0157022 (2016).
50. Kanehisa, M., Furumichi, M., Sato, Y. & Kawashima, M. Ishiguro-Watanabe, M. KEGG for taxonomy-based analysis of pathways and genomes. *Nucleic Acids Res.* **51**, D587–D592 (2023).
51. Kanehisa, M., Furumichi, M., Sato, Y., Matsuura, Y. & Ishiguro-Watanabe, M. KEGG: biological systems database as a model of the real world. *Nucleic Acids Res.* **53**, D672–D677 (2024).

Author contributions

CY S contributed to conceptualization, methodology, data management and writing - first draft. X M contributed to the investigation and participated in revision of the submitted article. RX Z contributed to software, and validation. ZH L and XC Z contributed to the Supervision. All authors read and approved the final version of the manuscript.

Funding

This research was supported by Jilin Province Science and Technology Development Project (YDZJ202301ZYTS127). This study was supported by Health Commission of Jilin Province (Project No. 2024B001).

Declarations

Competing interests

The authors declare no competing interests.

Ethics approval

Animal experiments received approval from Yanbian University's Ethics Committee (Programme No. YD20241014007). All animal operations were conducted in accordance with relevant guidelines and regulations. All methods are reported in accordance with ARRIVE guidelines.

Additional information

Supplementary Information The online version contains supplementary material available at https://doi.org/10.1038/s41598-025-94306-5.

Correspondence and requests for materials should be addressed to X.Z.